

Estimation of Neocortical Serotonin-2 Receptor Binding Potential by Single-Dose Fluorine-18-Setoperone Kinetic PET Data Analysis

Marie-Christine Petit-Taboué, Brigitte Landeau, André Osmont, Isabelle Tillet, Louisa Barré and Jean-Claude Baron
CYCERON, INSERM U320, Centre François Baclesse, CEA DSV/DPTE and IUT of Caen/University of Caen, Caen, France

Because it satisfies most of the characteristics required to quantify in vivo neocortical serotonin-2 (5HT₂) receptors, ¹⁸F-setoperone was selected for use in PET estimation of the neocortical 5HT₂ binding parameters in baboons according to a single-dose paradigm. **Methods:** The neocortical binding potential (i.e., B_{max}/K_D or the k₃/k₄ ratio) was assessed by three different methods, with the cerebellum taken as the reference structure in all instances. Method 1 was based on a Logan-Patlak graphical analysis of both cerebellar and neocortical data, which allows estimation of the neocortical k₃/k₄ ratio; it required a separate estimation of k₅ and k₆ from classical nonlinear least-squares (NLSQ) three-compartment modeling of cerebellar data. Method 2 was an original combination of a four-compartment Logan-Patlak procedure for neocortical data and an NLSQ three-compartment procedure for cerebellar data, allowing the neocortical k₃/k₄ ratio to be obtained directly. In Method 3, an NLSQ three-compartment procedure was applied to cerebellar data and an NLSQ four-compartment procedure to neocortical data, allowing separate determinations of k₃ and k₄ for the neocortex and, in turn, the k₃/k₄ ratio. **Results:** In all three methods, the arterial plasma input function was corrected for the presence of ¹⁸F-metabolites, and the vascular fraction was either fitted or fixed. Statistical analysis showed no significant difference among the k₃/k₄ values obtained from the three methods. Method 3 was the least stable because of an occasional poor NLSQ four-compartment fit on neocortical data. Method 2 provided the least cumbersome estimate of the k₃/k₄ ratio and was found easy and accurate for generating parametric maps of the 5HT₂ binding potential. **Conclusion:** This method might be useful in clinical investigations to provide quantitative assessment of receptor binding potential. In semiquantitative investigations, the neocortical-to-cerebellum pseudoequilibrium ratio may be adequate, as suggested by the significant correlations with measured k₃/k₄ ratios found here.

Key Words: serotonin-2 receptors; PET; compartmental models; graphical analysis

J Nucl Med 1996; 37:95-104

Alterations in serotonergic transmission involving the serotonin-2 (5HT₂) receptors could play a role in disorders of higher cortical functions, such as Alzheimer's disease (1). In vivo investigations of the 5HT₂ receptors by PET have been limited by lack of an adequate tracer. The short half-life of ¹¹C has considerably limited studies using ¹¹C-labeled antagonists, such as methyl-spiperone and ketanserin (2,3). PET studies with spiperone derivatives labeled with the 2-hr half-life positron emitter ¹⁸F (4,5) have been characterized by rapid dissociation and high nonspecific binding. Both in vitro and ex vivo autoradiographic investigations with ¹⁸F-setoperone (6), an antagonist with a high affinity for the 5HT₂ receptors, have provided encouraging results. In both baboons and humans in vivo, Blin et al. (7,8) demonstrated that this radioligand was

suitable for PET studies of cortical 5HT₂ receptors. Thus, although ¹⁸F-setoperone labeled both the 5HT₂ and the D2 receptors in the striatum, displacement experiments showed that it bound only to the 5HT₂ receptors in the cerebral cortex, probably because the neocortical D2 receptor density is so low in primates as to be essentially undetectable either in vitro or in vivo (9,10). More recently, ¹⁸F-altanserin has also been proposed for PET investigations of 5HT₂ receptors (11).

The in vivo distribution of ¹⁸F-setoperone in both baboons and humans has been previously characterized only by descriptive tracer kinetic experimental designs. Fluorine-¹⁸F-setoperone, however, has ideal features for quantification of neocortical 5HT₂-specific binding for three main reasons:

1. It is a lipophilic compound that readily passes, and thus rapidly equilibrates, across the blood-brain barrier.
2. Fluorine-18-labeled metabolites are relatively polar and do not cross this barrier to any meaningful extent (12).
3. The cerebellum is known to be virtually devoid of 5HT₂ receptors in primates (13,14) and thus should provide a convenient structure of reference to estimate the nonspecifically bound ligand concentration.

Furthermore, earlier PET studies by Blin et al. (7,8) in both baboons and humans reported no displaceable ¹⁸F-setoperone binding in the cerebellum. Using the cerebellum ¹⁸F-setoperone concentration as an index for the free and nonspecifically bound ligand concentration in the cerebral cortex, these investigators showed that specific binding is reversible, and a state of "pseudoequilibrium" (i.e., a stable neocortex/cerebellum ratio) is reached within 1 hr after tracer injection. Despite these favorable features for quantification, only semiquantitative assessments of neocortical specific binding of ¹⁸F-setoperone, as determined by the region-to-cerebellum "ratio method" (7,8) or region minus cerebellum subtraction method (1), have been performed so far. The aims of this study therefore were to assess the feasibility of estimating neocortical 5HT₂ binding potential (i.e., B_{max}/K_D) (15) in single-dose ¹⁸F-setoperone experiments and to determine how the simple ratio method relates to this quantitative determination by systematic investigations in baboons. A preliminary account of these results has been presented previously (16).

MATERIALS AND METHODS

Radiochemistry

Fluorine-18-setoperone was synthesized using the method described by Crouzel et al. (17). Setoperone was labeled by nucleophilic substitution of an nitrous oxide (N₂O) group by ¹⁸F. Reactivity of ¹⁸F was increased with Kriptofix 2.2.2. (Aldrich) and potassium carbonate. After evaporation, K¹⁸F reacted with a nitro derivative of setoperone. The product was purified by high-performance liquid chromatography.

Received Nov. 12, 1994; revision accepted May 15, 1995.
For correspondence or reprints contact: Jean-Claude Baron, MD, INSERM U320, Cyceron, BP5229, 14074 Caen Cedex, France.

Animal Preparation

Tracer dose experiments were carried out in 12 young adult baboons (*Papio anubis*) with the following protocol, chosen for its lack of interference with 5HT₂ binding on the basis of in vitro data (18,19). The animals were initially sedated with the short-acting barbiturate methohexital (Brietal, 20 mg/kg body weight [b.w.] intramuscularly), which was relayed by an intravenous injection of etomidate (Hypnomidate, 3 mg/kg b.w.), potentiated by an infusion of clonidine (Catapressan, 75 µg i.v. over 10 min), and muscular relaxation was achieved with atracurium (Tacurarium, 0.5 mg/kg b.w.). Anesthesia was subsequently maintained with etomidate (0.3 mg/kg/hr, i.v. infusion), atracurium (0.75 mg/kg/hr, i.v. infusion) and artificial ventilation with a N₂O–oxygen mixture (2:1).

Venous catheters were placed in both femoral veins for administration of physiological fluids, anesthetic drugs and ¹⁸F-setoperone. Arterial catheters were placed percutaneously in both femoral arteries to allow blood sampling for radioactivity measurement, determination of the physiological parameters and monitoring of arterial pressure. The rectal temperature was monitored and kept within normal limits with heating blankets. The baboon's head was carefully positioned in the field of view of the PET camera with a specially designed headholder equipped with ear bars and a submandibular blocking bar so that the scan slices were parallel to the canthomeatal line. An anteroposterior skull radiograph was obtained to ensure correct positioning of the ear bars within the bony portion of the external auditory canals. This procedure allowed both reproducible intra-animal and standard interanimal positioning.

Positron Emission Tomographic Measurements

PET data were acquired with the seven-slice LETI TTV03 time-of-flight camera (intrinsic resolution: 5.5 × 5.5 × 9 mm [x, y, z, respectively]). The cuts were made to parallel the canthomeatal line from -27 to +45 mm relative to this line. After transmission scanning with ⁶⁸Ge, a bolus of ¹⁸F-setoperone (injected dose 6.09 ± 1.11 mCi [mean ± s.d.], specific radioactivity range 135–1635 mCi/µmole, mean ± s.d. 742.5 ± 601 mCi/µmole) was injected. PET acquisition with the list mode procedure started from the beginning of the bolus injection (t₀) and lasted 120 min. Data were reconstructed with the following image frame sequences: 9 × 16-, 5 × 30, 5 × 60, 6 × 300 and 4 × 1200 sec. Initial (0–2 min) 2-sec head counts were also recorded (20) to fit the brain/arterial shift of ¹⁸F increase (21). The PET data were automatically corrected for ¹⁸F decay, and scatter was empirically corrected according to the technique of Bendriem et al. (22).

Quantification of Arterial Radioactivity and Fluorine-18-Labeled Metabolites

Arterial sampling started simultaneously with PET acquisition (i.e., at start of radiotracer injection). About 12 samples (~1 ml) were withdrawn in the first minute and about 10 samples (~1 ml) at increasing intervals until the end of the study. Radioactivity in whole blood and total plasma, corrected for ¹⁸F decay, were measured in nanocuries per milliliter with a gamma counter cross-calibrated with the PET camera.

The plasma input function was corrected for the presence of ¹⁸F-metabolites estimated by thin-layer radiochromatography (TLRC), as previously described by Blin et al. (12). Only two to five determinations were possible in each experiment. Briefly, plasma was deproteinated with methanol. After evaporation of the supernatant, the residue was dissolved in a mixture of acetonitrile and methanol and analyzed by TLRC with dichloromethane/methanol/ethylamine (100:12:0.2 vol) as the migration solvent. This allowed expression of the results in terms of percent of unchanged ¹⁸F-setoperone for each determination. Using weighted nonlinear interpolation across the initial 28 determinations (8 PET

studies), we defined a standard metabolite correction curve that was used for all further analyses. Using the same method of TLRC, we were able to document the absence of detectable ¹⁸F-metabolites in either the cortical or the cerebellar samples obtained in two animals killed 2 hr after ¹⁸F-setoperone injection (data not shown), which confirm indirect evidence of Blin et al. (12). Arterial whole-blood curves were used to determine the vascular fraction (see Data Analysis).

Determination of Regions of Interest

For each PET frame, the cerebellar data were obtained from averaging across all the pixels surrounded by two circular regions of interest (ROIs) (1-cm diameter) placed on the cut canthomeatal + 9 mm on the basis of corresponding CT scan cuts obtained in the same canthomeatal positioning by means of the same ear bar head frame (20,23). Whole cerebral cortex kinetic data were taken as an average of 90 voxels (28 ROIs) of the same shape and size on each side of the brain and placed over three adjacent PET planes (CM + 9 mm, CM + 21 mm and CM + 33 mm). Radioactivity concentration in these regions was calculated for each sequential scan and plotted versus time.

THEORETICAL AND DATA ANALYSES

Model Configuration

The kinetics of ¹⁸F-setoperone in the neocortex and cerebellum were modeled according to one of the two classic configuration models illustrated in Figure 1. In a simplified three-compartment model with free (F) and nonspecific binding (NS) compartments combined (Fig. 1A), the constants are K₁ (in milliliters per gram per minute; for transport into tissue space); k'₂ (dissociation from the combined F and NS compartments); k'₃ (forward rate constant of association to S, the 5HT₂ receptor compartment); k₄ (dissociation from S); and V_f (the vascular fraction, in milliliters per milliliter). In the full four-compartment model (Fig. 1B), the constants are K₁ (in milliliters per gram per minute) and k₂ for transport into and out of the free ligand compartment; k₃ and k₄ for binding to and dissociation from the 5HT₂ receptors; and k₅ and k₆ for binding to and dissociation from the NS compartment (k₂ – k₆, min⁻¹). In both configurations, the assumption is made that the cerebellum can serve as a reference tissue to assess the exchanges among plasma, free ligand and nonspecific binding in the neocortex (see below). In all models, V_f, which represents the vascular fraction in the block of tissue under consideration, was determined by fitting, unless specified otherwise. The neocortical binding potential was calculated as the k₃/k₄ ratio (15). The fraction of the ligand available either for binding to the receptors or for transport back to plasma is represented by the term 1/(1 + k₅/k₆) (24), which is equivalent to the term f₂ used by Mintun et al. (15).

General Modeling Strategy

The modeling strategy to quantify the neocortical 5HT₂ receptor binding potential used three different approaches (Fig. 2).

Method 1. Both the cerebellar and cortical datasets were analyzed with the classic Logan-Patlak graphical method [Logan et al. (25)] resulting in the k'₃/k₄ ratio for the neocortex. Then, by the classic nonlinear least-squares (NLSQ) fitting of cerebellar data, we determined k₅ and k₆ and, in turn, the k₃/k₄ ratio for the cortex (because k'₃/k₄ = {[1/1 + k₅/k₆] × (k₃/k₄) (24).

Method 2. We used an original four-compartment Logan-Patlak graphical analysis of cortical data, which allowed direct estimation of the k₃/k₄ ratio (with a prior three-compartment NLSQ procedure for cerebellar data, which allowed estimation of K₁/k₂ and k₅/k₆ [see later]).

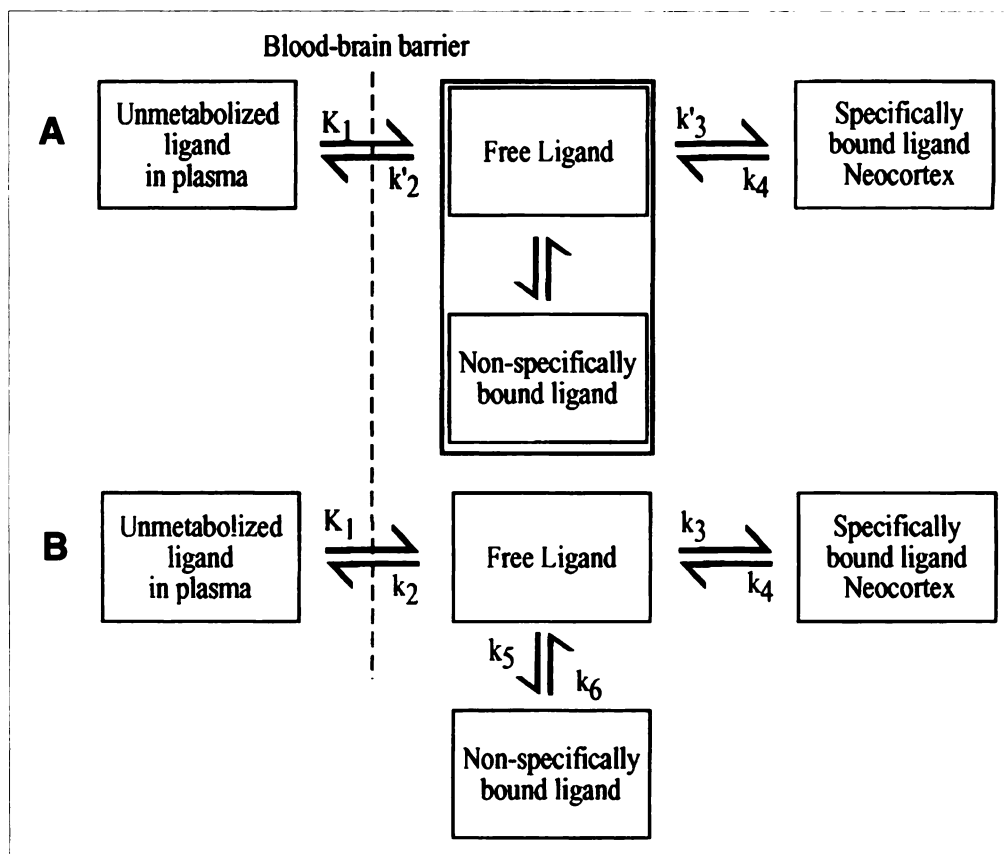


FIGURE 1. Compartmental model describing ^{18}F -setoperone behavior in the brain. (A) Simplified three-compartment model that combines the free and the nonspecifically bound ligand; the rate constants are K_1 , k_2 , k_3 and k_4 . (B) Full four-compartment model in which the exchange of ^{18}F -setoperone among the four compartments is described by rate constants K_1 and k_2 to k_6 .

Method 3. The neocortical data were fitted using a classical NLSQ procedure according to a four-compartment model (Fig. 1B), with the NLSQ procedure for cerebellar data providing K_1/k_2 , k_5 and k_6 . This approach provided k_3 and k_4 separately, from which the k_3/k_4 ratio was then calculated.

Determination of k_3/k_4 (Method 1)

The kinetics of ^{18}F -setoperone in the neocortex and cerebellum were modeled according to the model illustrated in Figure 1A by linear graphical analysis developed by Logan et al. (25), hereafter referred to as the Logan-Patlak plot. In this procedure, the integrated tissue activity from time zero to time T (corrected for intravascular tracer with a fixed V_f) is plotted against the corresponding integrated metabolite-corrected plasma time-activity data, with both quantities normalized to tissue activity at time T.

The value for V_f was taken as 0.04 [mean value of the cerebellar blood volume as measured in our laboratory in normal baboons with the same PET methodology and anesthetic regimen (26)]. When a state of pseudoequilibrium is reached, the plot becomes linear. Assuming that receptor binding is absent from the cerebellum (i.e., $k_3 = k_4 = 0$), the cerebellar time-activity data were analyzed according to a two-compartment model (i.e., plasma and F + NS combined); in this case, the slope of the asymptote equals K_1/k_2 .

Assuming that the neocortex corresponds to a three-compartment model (i.e., plasma, combined F + NS and S), the slope of the asymptote equals $(K_1/k_2) \times (1 + k_3/k_4)$. Assuming a similar K_1/k_2 ratio and similar k_5 and k_6 values than in the cerebellum in all instances (15,27,28), the ratio k_3/k_4 for the neocortex can easily be

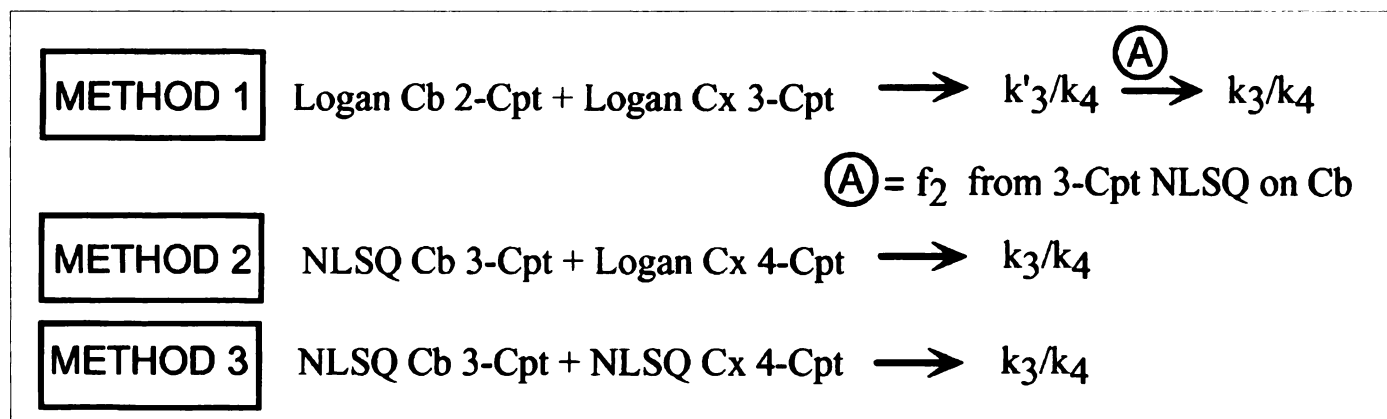


FIGURE 2. The three different methods for determination of ^{18}F -setoperone neocortical binding potential (k_3/k_4). Cb = cerebellum; Cx = neocortex; NLSQ = nonlinear least-squares fit; Cpt = compartment.

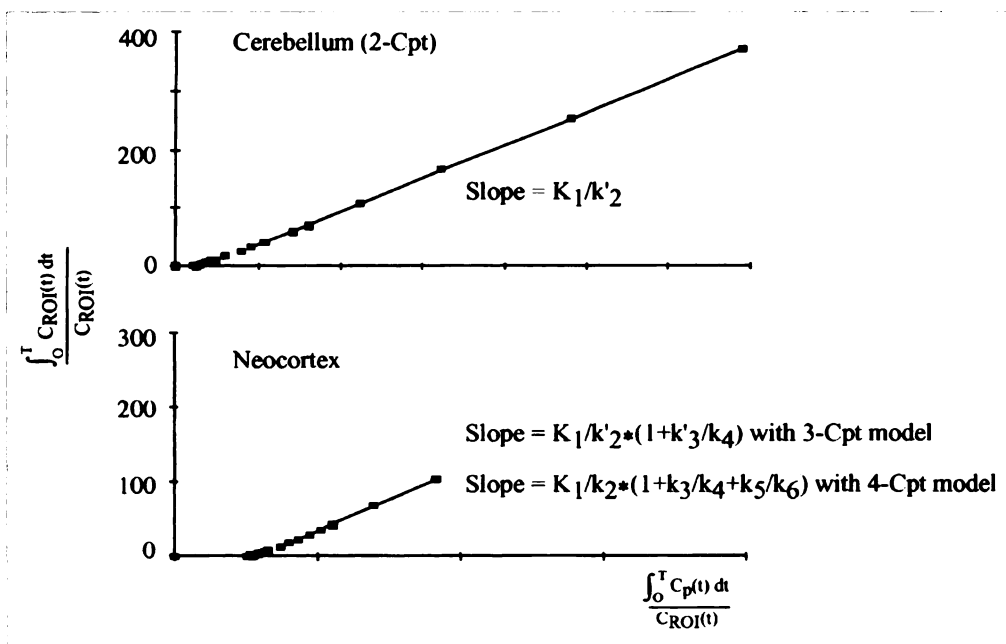


FIGURE 3. Logan-Patlak graphical analysis of the time-activity data from the cerebellum (two-compartment) and neocortex (three- and four-compartment) in the same baboon. $C_p(t)$ = intact ^{18}F -setoperone arterial plasma input function; $C_{ROI}(t)$ = radioactivity at time t in the region of interest.

obtained by dividing the Logan-Patlak neocortical slope by the corresponding cerebellar slope and subtracting 1 from the result of this division.

Determination of k_3/k_4

Method 1. To estimate k_5 and k_6 , the cerebellar data were fitted to a three-compartment model (fitted parameters K_1 , k_2 , k_5 , k_6 and V_f) (Fig. 2). The model time-activity function $C(t)$ was calculated as the sum of convolution integrals determined by the different parameters, the ^{18}F -metabolite-corrected plasma function and the ^{18}F whole-blood input function. Optimal values of the model parameters were obtained with a Marquardt NLSQ minimization procedure (29). To determine optimal start-of-fit values, the cerebellar data were first fitted with a wide range of starting fit values by changing each parameter's starting value in a systematic way while keeping the others fixed. The fixed parameters were then plotted as a function of the corresponding starting values. Stability of all fitted parameters was excellent over a greater than 8- to 10-fold range for each of the initial starting values, which were finally set as $K_1 = 0.25 \text{ ml} \cdot \text{g}^{-1} \cdot \text{min}^{-1}$, $k_2 = 0.12$, $k_5 = 0.05$, $k_6 = 0.035$ ($k_2 - k_6$ [min^{-1}]) and $V_f = 0.04$ and which represent the average of the median of the stable parts across the eight initial studies. Using the values of k_5 and k_6 from the same baboon to determine the fraction $1/1 + k_5/k_6$, the ratio k_3/k_4 for neocortex was then easily obtained from knowledge of k'_3/k_4 .

Method 2. The cortical data were analyzed according to the Logan-Patlak plot (Fig. 2). Using a four-compartment model (i.e., distinguishing plasma, F, NS and S as described in Fig. 1B), the slope of the plot now equals $(K_1/k_2) \times [1 + (k_3/k_4) + (k_5/k_6)]$. The k_3/k_4 ratio was easily determined from knowledge of the ratios K_1/k_2 and k_5/k_6 provided by the NLSQ procedure (three-compartment) for cerebellar data from the same baboon, with the same assumptions as before (15,27,28).

Method 3. Analysis of neocortical 5HT₂ binding to receptors was performed by a NLSQ fit on the basis of a classical four-compartment model (fitted parameters K_1 , k_3 , k_4 , V_f , with K_1/k_2 , k_5 and k_6 fixed at the three-compartment cerebellar values of the same baboon, obtained by a three-compartment NLSQ procedure for cerebellar data) (Fig. 2). The neocortical data were fitted using as the initial value for K_1 that estimated by the three-compartment NLSQ procedure for the same baboon's cerebellar data, and for k_3

and k_4 the values of 0.20 and 0.09, respectively, determined from stability tests according to the procedure previously described for the cerebellum. The k_3/k_4 ratio was calculated from the separately estimated k_3 and k_4 values.

Correlations with Neocortical-to-Cerebellar Ratios

We evaluated the relationships between the k_3/k_4 ratios obtained from Methods 1–3 and the corresponding neocortical/cerebellar (C_x/C_b) ratios obtained from the same ROIs, which are assumed to provide a semiquantitative index of specific binding (namely, $C_x/C_b = f_2(B_{\text{max}}/K_D) + 1$ (30)). The C_x/C_b ratio values were calculated for each baboon from the time-activity curves of neocortex and cerebellum used for modeling for selected PET frames (i.e., 10, 20, 30, 50, 60, 90 and 110 min and the mean 50–110 min). These values were then compared with each set of corresponding values for k_3/k_4 obtained from each of the three fitting methods. Correlations were assessed with the nonparametric Spearman rank test.

RESULTS

Logan-Patlak Plots

Figure 3 illustrates a typical example of the graphical analysis applied to the cerebellum (two-compartment) and cortical (three-compartment) time-activity data from the same baboon. In all cases, visual analyses showed clear-cut linearity of the final parts of the plots, with linearity beginning at about $t \sim 10$ min, for both structures. The slopes were automatically determined in all baboons by linear regression on all values for $t > 10$ min.

Individual values of the slopes obtained for the neocortex and cerebellum and the corresponding k'_3/k_4 ratios (Method 1) are reported in Table 1. As expected, the slopes were greater for the neocortex than for the cerebellum. The k'_3/k_4 ratios ranged from 1.20 to 2.64.

Cerebellum NLSQ

Figure 4A shows a typical example of fit of the cerebellar time-activity data by both two- and three-compartment models. As clearly illustrated in this typical example, the fit of the data was consistently better with the three-compartment model. In one baboon (no. 12), the visual result of the fit (with either a

TABLE 1
Individual and Mean (\pm s.e.m.) Slopes and k_3/k_4 Ratios from Graphical Analysis (Logan-Patlak Method) of Cerebellar and Neocortical Data

Baboon no.	Cerebellum slope	Neocortex slope	k_3/k_4 (Method 1)
1	2.77	6.52	1.35
2	2.41	7.76	2.22
3	2.97	8.49	1.86
4	4.00	9.89	1.47
5	2.58	5.30	2.05
6	2.37	5.93	1.50
7	2.41	6.42	1.66
8	2.91	6.41	1.20
9	2.19	6.12	1.80
10	1.16	4.20	2.64
11	0.99	2.75	1.85
12	1.58	4.55	1.88
Mean \pm s.e.m.	2.36 \pm 0.25	6.20 \pm 0.58	1.73 \pm 0.12

TABLE 2
Individual and Mean (\pm s.e.m.) AIC Values for Two-Compartment and Three-Compartment NLSQ Fit on Cerebellar Data

Baboon no.	NLSQ Two-Compartment	NLSQ Three-compartment
1	180	127
2	187	136
3	170	117
4	180	155
5	147	91
6	228	139
7	149	111
8	147	130
9	175	120
10	170	133
11	192	138
Mean \pm s.e.m.	175 \pm 7	127 \pm 5*

*Significantly lower than with two-compartment NLSQ; $p < 0.001$ by paired t-test.

AIC = Akaike Information Criteria.

two- or three-compartment model) was not acceptable, and this animal was therefore excluded from all further analyses. The mean (\pm s.e.m.) Akaike information criteria (AIC) (31) values for the 11 remaining animals were significantly lower with the 3- than with the two-compartment model (Table 2), suggesting that the F and NS 18 F-setoperone compartments may not be in rapid equilibrium and thus need to be kinetically separated with

a three-compartment model. The individual and mean estimates of the transfer coefficients obtained by three-compartment modeling of cerebellar data are shown in Table 3. Both the K_1 values and the measured K_1/k_2 ratios from Baboons 10 and 11 were notably different from the other animals, with the latter inferior to unit. These studies were therefore excluded from all further analyses.

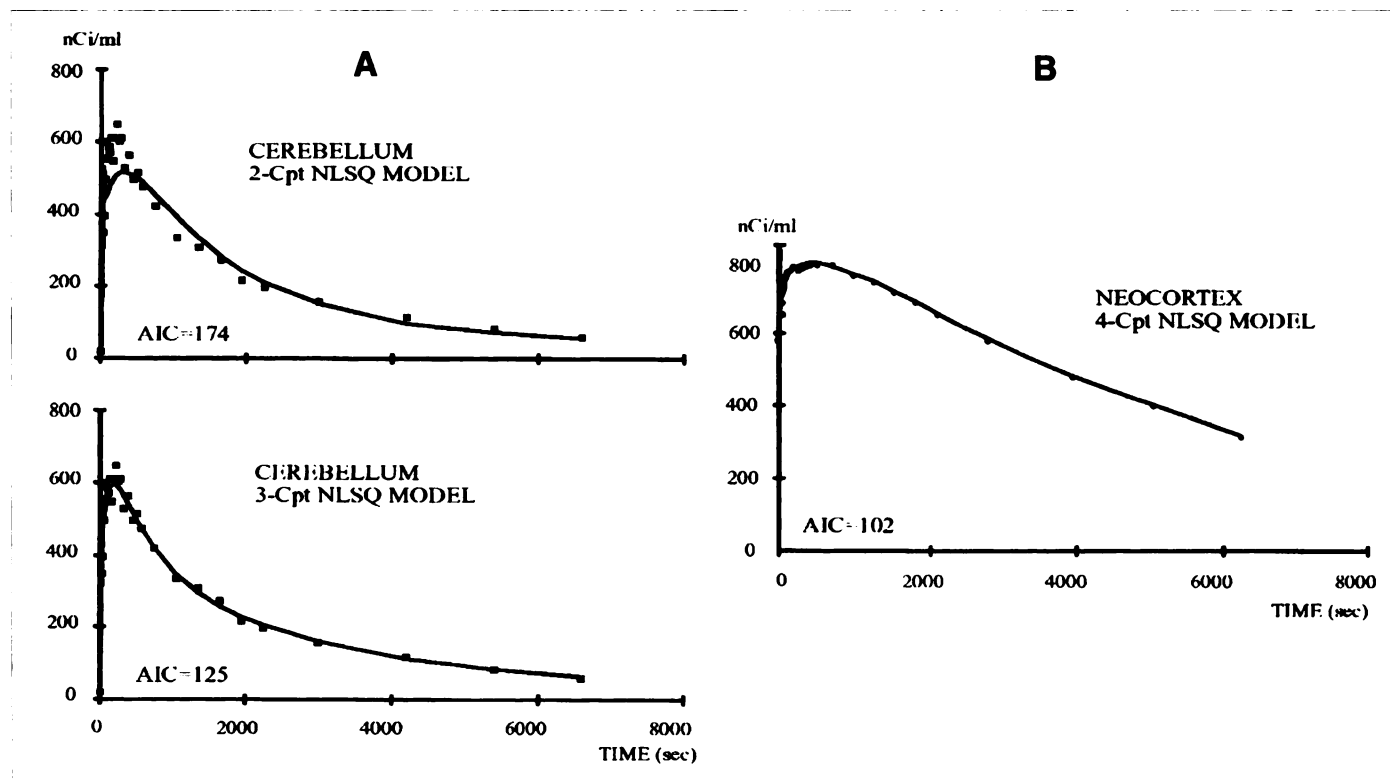


FIGURE 4. (A) NLSQ fit on cerebellar data according to a two-compartment model (top) and a three-compartment model (bottom) show considerably better fit with the latter than with the former. Also shown are the Akaike information criteria (AIC), which decreased from 175 to 127 with the three-compartment compared with the two-compartment model and is in agreement with the visual impression of better fit with the former. (B) Illustrative neocortical time-activity curve from the same baboon and same PET session show an extended buildup phase as well as slower washout than in the cerebellum. Also shown is the excellent fit with a four-compartment NLSQ model (AIC = 102).

TABLE 3
Individual and Mean (\pm s.e.m.) Estimates of Transfer Coefficients (K_1 and k_2-k_2) and Vascular Fraction (V_d) by NLSQ for Cerebellar Fluorine-18

Baboon no.	K_1 (ml/g · min)		k_2 (min^{-1})	
	Cb	Cx	Cb	Cx
1	0.179	0.160	0.084	0.081
2	0.266	0.251	0.163	0.154
3	0.251	0.222	0.139	0.124
4	0.220	0.203	0.084	0.078
5	0.178	0.217	0.106	0.129
6†	0.225	0.198	0.200	0.095
7	0.212	0.203	0.135	0.129
8	0.198	0.213	0.084	0.090
9	0.140	0.151	0.091	0.097
10	0.115	ND	0.153	ND
11	0.123	ND	0.280	ND
Mean \pm s.e.m.	0.190 \pm 0.014	0.202 \pm 0.011	0.156 \pm 0.025	0.109 \pm 0.009

Neocortical k_3/k_4 Ratios from Methods 1 and 2

The individual and mean (\pm s.e.m.) values for the k_3/k_4 ratios obtained according to Methods 1 and 2 with the graphical analysis combined with the three-compartment NLSQ procedure for cerebellar data (nine animals) are shown in Table 4 (which also shows results from Method 3 [see next section]). The individual values were fairly consistent among the two methods, except for one animal (Baboon 5). Also, there was substantial interanimal variability in k_3/k_4 ratios for either method (coefficients of variation [COVs] are 25% and 29% for Methods 1 and 2, respectively).

Neocortical NLSQ (Method 3)

A four-compartment NLSQ procedure was performed for the neocortical data from the nine baboons in which the NLSQ procedure on the cerebellar data provided consistent results. The individual and mean estimates for the transfer coefficients obtained from this analysis are shown in Table 3 and illustrated in Figure 4B. Rapid convergence and good fit were obtained in all nine animals except Baboon 6. For this baboon, it was not possible to fit the cortical data using the values K_1 (as the initial fitting estimate) and K_1/k_2 (fixed ratio) obtained from the three-compartment NLSQ procedure for this animal's cerebellar data; however, the fit was good if the initial fitting value used for the cerebellum three-compartment NLSQ procedure (i.e., $K_1 = 0.25$, with $K_1/k_2 = 2.08$) was used, but the estimates for k_3 and k_4 markedly differed from the results for the other animals (see Table 3).

The individual k_3/k_4 ratios obtained with Method 3 are shown in Table 4. The COV was 35%, but this is largely explained by the results from neocortical modeling in Baboon 6, which were spurious (see above). If this animal is excluded, the COV for the NLSQ method becomes 25%, comparable to that obtained with the two other methods. Statistical analysis by multivariate analysis of variance (MANOVA) showed no significant difference among the three methods (either including or excluding Baboon 6).

Pixel-by-Pixel Imaging of k_3/k_4

Parametric images of the neocortical k_3/k_4 ratio were obtained by applying a four-compartment Logan-Patlak analysis (Method 2) on a pixel-by-pixel basis to the three PET planes of interest. The graphical method for the 120-min ^{18}F -setoperone dynamic data was used by plotting $\int_0^T \text{Pixel}(t) dt/\text{pixel}(T)$ versus $\int_0^T \text{Cp}(t) dt/\text{pixel}(T)$ on the time-activity f curves of each pixel (32), where $\text{pixel}(T)$ is the radioactivity in the pixel at time T . Using the K_1 , k_2 , k_3 and k_4 values previously determined from the NLSQ method for cerebellar ROI data (Method 2), we were able to map the distribution of the neocortical k_3/k_4 ratios on a pixel-by-pixel basis (Fig. 5). To validate this method, we calculated from these parametric images a mean k_3/k_4 value for all pixels contained in the neocortical ROIs used in the previous procedures and compared the values obtained with the results of the graphical analysis (Method 2) previously obtained for the same ROIs. The mean k_3/k_4 values for the two methods were 2.45 and 2.39, respectively (no significant difference, Student's paired t-test). The COV of neocortical k_3/k_4 in these ROIs was about 20%, which was considered acceptable. The k_3/k_4 values were consistently higher in the frontal and occipital cortices compared with the temporal and parietal cortices, as expected for the 5HT₂ receptors (Fig. 5).

Neocortical to Cerebellar

Table 5 shows the Spearman coefficients of correlation between the Cx/Cb ratios (measured from various PET frames and corresponding k_3/k_4 values determined from each of the three models in nine baboons). Statistically significant positive correlations ($p < 0.01$) were found between the quantitative determinations of k_3/k_4 and the Cx/Cb ratios for all times, regardless of the method used to determine k_3/k_4 ; but on average, the lowest correlation coefficients were obtained for the time ($t = 10$ min).

DISCUSSION

The results of the present study demonstrate two main findings: (a) that quantitative estimates of in vivo neocortical 5HT₂ receptor binding potential can be determined using the

TABLE 3
 Setoperone Time-Activity Data (Three-compartment Model) in 11 Baboons and Neocortex Fluorine-18-Setoperone Time-Activity Data (Four-compartment Model) in Nine Baboons

k_3 (min^{-1}) Cx	k_4 (min^{-1}) Cx	k_5 (min^{-1}) Cb*	k_6 (min^{-1}) Cb*	V_f (ml/ml)	
				Cb	Cx
0.248	0.135	0.013	0.027	0.056	0.040
0.225	0.067	0.032	0.047	0.035	0.032
0.373	0.122	0.038	0.057	0.037	0.039
0.493	0.205	0.017	0.030	0.048	0.040
0.150	0.067	0.019	0.024	0.083	0.063
0.022	0.027	0.023	0.019	0.077	0.073
0.227	0.089	0.032	0.051	0.040	0.031
0.164	0.111	0.005	0.012	0.033	0.044
0.200	0.083	0.011	0.021	0.055	0.036
ND	ND	0.008	0.020	0.058	ND
ND	ND	0.075	0.028	0.044	ND
0.233 ± 0.047	0.101 ± 0.018	0.029 ± 0.007	0.032 ± 0.004	0.052 ± 0.005	0.044 ± 0.005

*Values obtained from NLSQ on cerebellar (Cb) data were used in the NLSQ procedure on neocortical (Cx) data from the same baboon.

†Reasonable four-compartment NLSQ fit on neocortical data was only obtained using, as initial fitting values, the starting fitting values used for the cerebellum; however, the estimates for the transfer rates were spurious—notably, k_4 was larger than k_3 .

ND = not determined (see Results).

^{18}F -setoperone single-dose kinetic PET experiment; and (b) that the binding potential can be accurately derived from an original combination of NLSQ fit on cerebellar data and simple Logan-Patlak graphical linearization procedures, thereby avoiding cumbersome and potentially unstable four-compartment modeling of neocortical data.

Although single-dose conditions, as initially proposed by Mintun et al. (15) preclude the calculation of B_{max} and K_D separately, the advantage of this logistically simple approach in our case was to avoid the administration of displacing amounts of 5HT₂ blockers. Indeed, such agents not only have untoward pharmacological effects, such as hypotensive effects and increase in slow-wave sleep (19), but this approach would also not be appropriate in neurobiologic paradigms that aim at measuring the sequential effects of brain lesions on the density and affinity of receptors (23) because large amounts of 5HT₂ blockers may induce secondary alterations in receptor density.

Although the three methods that we used provided consistent estimates of k_3/k_4 , Method 3, which entailed cumbersome

NLSQ fitting on both cerebellar and neocortical data provided the most variable results (COV = 35%), as a result of unstable estimates in one baboon. This problem, however, was not unexpected and is one well-known limitation of multicompartmental analysis of time-activity data (33,34). This serves to illustrate the usefulness of our approach, which combines a three-compartment NLSQ fit on cerebellar data and a Logan-Patlak plot on the neocortex (associated or not with a Logan-Patlak procedure on the cerebellum). Furthermore, to apply an NLSQ fit on neocortical data on a pixel-by-pixel basis would not only be cumbersome, but would presumably also further enhance the risk of spurious results. We show here the feasibility of applying our simple Logan-Patlak approach on a pixel-by-pixel basis to generate parametric imaging of neocortical binding potential.

In the present study, we used the cerebellum as the reference structure because it is virtually devoid of 5HT₂ receptors in primates (13,9), and ^{18}F -setoperone displaceable binding is undetectable in vivo in baboons (7). This approach is classic in PET studies when the single-dose experiment is the desired paradigm (15,27,25,33). To obtain adequate results from the different models, it was also necessary to correct the plasma input function for labeled metabolites of ^{18}F -setoperone (data

TABLE 4
 Individual and Mean (\pm s.e.m.) k_3/k_4 Ratios for Neocortical 5HT₂ Binding Obtained by Three Methods

Baboon no.	Method 1	Method 2	Method 3
1	2.02	1.80	1.83
2	3.73	3.08	3.36
3	3.09	2.70	3.05
4	2.28	2.22	2.40
5	2.36	1.36	2.23
6	3.31	3.07	0.81
7	2.71	2.46	2.56
8	1.69	1.31	1.48
9	2.75	2.42	2.42
Mean \pm s.e.m.	$2.66 \pm 0.23^*$	$2.27 \pm 0.23^*$	$2.24 \pm 0.28^*$

*No significant difference among the three methods (MANOVA).

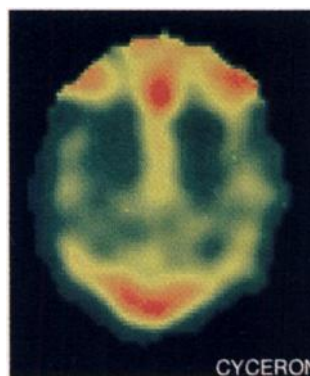


FIGURE 5. Parametric pixel-by-pixel images of neocortical k_3/k_4 obtained according to Method 2 (see Methods and Results), illustrated here for PET level (CM + 21 mm), that is, at the level of the corona radiata, and illustrating higher k_3/k_4 values in the frontal and occipital cortices.

TABLE 5

Correlation Coefficients for k_3/k_4 Ratio Values from Methods 1–3 and Neocortex/Cerebellum (Cx/Cb) Determined at Different Times after Administration of ^{18}F -Setoperone in Nine Baboons*

Method	Cx/Cb							
	10 min	20 min	30 min	50 min	70 min	90 min	110 min	50–110 min
1	0.87	0.93	0.97	0.99	0.98	0.97	0.97	0.97
2	0.92	0.96	0.98	0.98	0.97	0.94	0.95	0.94
3	0.91	0.94	0.95	0.91	0.89	0.90	0.93	0.91

*Spearman's rank correlations
 $p < 0.01$ for all correlations.

not shown). To perform this correction, we used a standard correction curve because it proved impossible to determine an accurate individual correction for each animal because only a limited number of samples could be processed. Adequate data, however, were available in six baboons, which allowed us to compare the results obtained with the standard correction curve with those obtained from individual determination. This comparison showed no significant difference in the results of modeling (data not shown).

Logan-Patlak Analysis

In Method 1, the graphical technique developed by Logan et al. (25) was applied to both the neocortical and cerebellar data and allowed us to determine directly the k_3/k_4 ratio by simply dividing the neocortical by the cerebellar slope. The k_3/k_4 ratios obtained in this way were fairly consistent among the different baboons (COV 20%). The slopes for both the cerebellum and neocortex became rapidly linear (for $t > 10$ min), although the last point at times tended to slightly deviate from linearity. This could reflect delayed entry of labeled metabolites in tissue. Thus, Blin et al. (12) reported a very slow brain penetration of the main ^{18}F -labeled metabolite of setoperone, which slowly diffused through the choroid plexus into the brain extracellular space. We, however, detected only the parent radioligand in tissue from two baboons killed 2 hr after ^{18}F -setoperone administration.

We have designed a method that combines a straightforward graphical analysis with a three-compartment NLSQ fit on cerebellar data to derive k_3/k_4 ratios for neocortical 5HT₂ binding. In Method 1, after the determination of k_3/k_4 just described, the estimation of k_5 and k_6 , and thus $1/1 + k_5/k_6$, from a three-compartment NLSQ procedure on cerebellar data allowed us to calculate k_3/k_4 , whereas in Method 2, the values for K_1 , k_2 , k_5 and k_6 obtained from a three-compartment NLSQ fit on cerebellar data were used in combination with a Logan-Patlak plot and a four-compartment model on neocortical data to determine k_3/k_4 . The k_3/k_4 values obtained from these two methods were not significantly different, and their COVs were of similar magnitude. Because the Logan-Patlak plots in Method 1 are based on a combined (F + NS) compartment, which we found not to be optimal on the basis of NLSQ fit results for cerebellar data, we would favor Method 2, which does not make this assumption.

Cerebellar Time-Activity Curve-Fitting Strategy

Regardless of the method used, the present paradigm relies on a compartmental analysis of cerebellar time-activity curves. The values of the fit with a two- and with a three-compartment model were compared to determine the most appropriate model configuration. Using the AIC criterion (31), the fit was significantly better with the three- than the two-compartment model,

suggesting that the F and NS compartments for ^{18}F -setoperone may not be in rapid equilibrium and thus must be kinetically separated with a three-compartment model. The NLSQ procedure on cerebellar data, however, failed to converge on a meaningful fit in 1 of 12 baboons. This presumably reflects the well-known problem of high sensitivity of the multicompartmental fitting paradigm to measurement errors in the time-activity curves for both tissue and input function (35). It might be suggested that the poor signal-to-noise ratio, due to rapid sampling in the initial part of the PET acquisition procedure, could explain such results; however, even reconstructing 30-sec images from our list-mode PET data did not improve the fit in this baboon. Inaccuracies in the determination of the arterial input function could also be involved. In the present study, the arterial blood samples were in rapid sequence in the early period after radioligand administration, but the exact peak may still have been missed. In the remaining animals, the results of fitting were satisfactory (Table 3). The values for $1/1 + k_5/k_6$ obtained by NLSQ fitting on cerebellar data ranged from 0.45 to 0.70, which are coherent with values previously reported for other ligands (28). For unknown reasons, however, the K_1/k_2 ratios in Baboons 10 and 11 were different from the other animals and were less than 1 (0.51 and 0.75, respectively), which led us to exclude these two animals from further analyses to have comparable results for the analysis of the neocortical data.

Neocortex Time-Activity Curve-Fitting Strategy (Method 3)

The application of a multicompartmental analysis to ^{18}F -setoperone neocortical time-activity data was based on the underlying assumptions that the rate constants for setoperone transfer into and out of brain tissue and between free and nonspecifically bound compartments estimated in the cerebellum, reliably reflected those of the neocortex. Thus, the values of k_3 and k_4 for neocortex were determined: (a) with the ratio K_1/k_2 held constant at that value estimated in the same baboon's cerebellum, whereas the individual value of K_1 was allowed to vary; and (b) with the individual k_5 and k_6 fixed at the values determined in the same baboon's cerebellum (15,27). The ratio K_1/k_2 is assumed to be uniform not only between the neocortex and cerebellum but also within the neocortex from region to region (and from pixel to pixel in the parametric image generation). Although this assumption is probably reasonable in normal tissue, the ratio K_1/k_2 may vary unpredictably in pathologic situations (25), although meaningful changes would be expected only when tissue chemistry is severely disrupted (e.g., cerebral infarction, tumors). With the use of Method 3, the mean value for k_3/k_4 was 2.24, consistent with the findings from the other two methods and indicating that the simpler methods provided adequate results. As stated earlier, however, the COV

with Method 3 (35%) was the highest of the three methods. This COV for the k_3/k_4 ratio was nevertheless lower than that for k_3 and k_4 separately (58% and 51%, respectively) (Table 3). Logan et al. (25) also reported similar observations for ^{11}C -carfentanil, suggesting that the binding potential is a relatively more stable parameter than either k_3 or k_4 alone. In one of our nine baboons, the four-compartment fit of neocortex data resulted in spurious values because of the inherent instability of multicompartmental fitting alluded to previously. In addition to the problems regarding data noise and inaccuracies in correction for ^{18}F -setoperone metabolization, previously discussed, another factor may relate to the vascular fraction because it was an additional parameter to be fitted in this study. Additional fitting, however, was also done with the vascular fraction fixed at the value found for the cerebellum, but this did not improve the results of the fit, and the variance in the estimated rate constants were not meaningfully different (data not shown). In the present study, the values for V_f obtained when this parameter was fitted, were within the normal range, as determined previously in normal baboons both for neocortex and cerebellum (26).

Parametric Imaging

We found that parametric imaging was feasible on a pixel-by-pixel basis with Method 2, yielding images of k_3/k_4 that did not contain spurious noise. The results showed k_3/k_4 values higher in the frontal and occipital cortices than in the temporoparietal cortices. These results agree with the PET findings of Blin et al. (12) and with in vitro 5HT_2 receptor densities (13,14), and indicates that our approach involving Logan-Patlak plots on neocortical pixel data, combined with NLSQ fitting on cerebellar ROIs, should be useful for clinical applications.

Comparison with Ratio Method

The "ratio" approach has long been in use in the clinical setting because it requires neither blood sampling nor sequential PET data acquisition. Thus, it avoids the requirements of arterial catheterization and prolonged immobility of the patient and does not require cumbersome handling of both blood samples (i.e., centrifugation pipetting, gamma counting and determination of labeled metabolites) and PET data (especially dynamic image reconstruction and modeling procedures). This method, however, is only semiquantitative and relies on the assumption that the f_2 value is constant from subject to subject; It therefore needs to be validated for each radioligand before it can be generalized in the clinic. For we have shown ^{18}F -setoperone, that the neocortical-to-cerebellar ratios are correlated to the k_3/k_4 values with similar statistical significance across all times longer than 10 min, suggesting that a stable pharmacological pseudoequilibrium is reached after this time with ^{18}F -setoperone. This suggests that the ratio method for ^{18}F -setoperone is a reliable, semiquantitative index of the neocortical 5HT_2 binding potential for use in clinical investigations.

CONCLUSION

Our approach described here, which combines three-compartment modeling on cerebellar data and graphical analysis on cortical data, is advantageous because it is less cumbersome to apply, appears less sensitive to input function errors than full four-compartment modeling on neocortical data and provides adequate k_3/k_4 ratios. Furthermore, our method can be readily applied to generating parametric images of the binding potential on a pixel-by-pixel basis.

ACKNOWLEDGMENTS

We are particularly grateful to O. Touzani, A. Young and E.T. MacKenzie for animal anesthesia and PET experiments; P. Rioux and D. Speckel for statistical assistance; and J. Delforge for helpful discussions. We also thank the cyclotron, chemistry, computer and technical staffs of Cyceron.

REFERENCES

- Blin J, Baron JC, Dubois B, et al. Loss of brain 5-HT_2 receptors in Alzheimer's disease: in vivo assessment with positron emission tomography and ^{18}F -setoperone. *Brain* 1993;116:497-510.
- Wong DF, Wagner HN, Dannals RF, et al. Effects of age on dopamine and serotonin receptors measured by positron tomography in the living human brain. *Science* 1984;226:1393-1396.
- Baron JC, Samson Y, Comar D, Crouzel C, Deniker P, Agid Y. Etude in vivo des récepteurs sérotoninergiques centraux chez l'homme par tomographie à positons. *Rev Neurol* 1985;141:537-545.
- Arnett CD, Wolf AP, Shiue CY, et al. Improved delineation of human dopamine receptors using ^{18}F -N-methyl-spiperone and PET. *J Nucl Med* 1986;27:1878-1882.
- Coenen HH, Wienhard K, Stöcklin G, et al. PET measurements of D2 and S2 receptor binding of 3-N-(2- ^{18}F fluoroethyl)spiperone in baboon brain. *Eur J Nucl Med* 1988;14:80-87.
- Mazière B, Crouzel C, Venet M, et al. Synthesis, affinity and specificity of ^{18}F -setoperone, a potential ligand for in-vivo imaging of cortical serotonin receptors. *Nucl Med Biol* 1988;15:463-468.
- Blin J, Pappata S, Kiyosawa M, Crouzel C, Baron JC. Fluorine-18-setoperone: a new high-affinity ligand for positron emission tomography study of the serotonin-2 receptors in baboon brain in vivo. *Eur J Pharmacol* 1988;147:73-82.
- Blin J, Sette G, Fiorelli M, et al. A method for the in vivo investigation of the serotonergic 5-HT_2 receptors in the human cerebral cortex using positron emission tomography and ^{18}F -labeled setoperone. *J Neurochem* 1990;54:1744-1754.
- De Keyser J, Clayes A, De Backer JP, Ebinger G, Roels F, Vauquelin G. Autoradiographic localization of D1 and D2 dopamine receptors in the human brain. *Neurosci Lett* 1988;91:142-147.
- Farde L, Pauli S, Hall H, et al. Stereoselective binding of ^{11}C -raclopride in living human brain: a search for extrastriatal central D2-dopamine receptors by PET. *Psychopharmacology (Berlin)* 1988;94:471-478.
- Biver F, Goldman S, Luxen A, et al. Multicompartmental study of fluorine-18 altanserin binding to brain 5HT_2 receptors in humans using positron emission tomography. *Eur J Nucl Med* 1994;21:937-946.
- Blin J, Crouzel C. Blood-cerebrospinal fluid and blood-brain barriers imaged by ^{18}F -labeled metabolites of ^{18}F -setoperone studied in humans using positron emission tomography. *J Neurochem* 1992;58:2303-2310.
- Schotte A, Maloteaux JM, Laduron PM. Characterization and regional distribution of serotonin S_2 -receptors in human brain. *Brain Res* 1983;276:231-235.
- Pazos A, Probst A, Palacios JM. Serotonin receptors in the human brain: IV. Autoradiographic mapping of serotonin-2 receptors. *Neuroscience* 1987;21:123-139.
- Mintun MA, Raichle ME, Kilbourn MR, Wooten GF, Welch MJ. A quantitative model for the in vivo assessment of drug binding sites with positron emission tomography. *Ann Neurol* 1984;15:217-227.
- Petit-Taboué MC, Landeau B, Osmont A, et al. Estimation of cortical 5HT_2 receptor ($5\text{HT}_2\text{R}$) binding parameters from single dose ^{18}F -setoperone data in baboons: comparison of different methods [Abstract]. *J Cereb Blood Flow Metab* 1993;13(suppl 1):S795.
- Crouzel C, Venet M, Irie T, Sanz G, Boullais C. Labelling of a serotonergic ligand with ^{18}F : ^{18}F -setoperone. *J Lab Comp Radiopharm* 1988;25:403-414.
- Leysen JE, Niemegeers CJE, Van Nueten JM, Laduron PM. Tritiateal ketanserin (R 41 468), a selective ^3H -ligand for serotonin binding sites. *Mol Pharmacol* 1981;21:301-314.
- Leysen JE, Pauwels PJ. Serotonin receptor regulation: implications for drug action. In: Racagni G, et al. (eds.). *Biological psychiatry*, vol. 2. Amsterdam: Elsevier; 1991: 702-705.
- Miyazawa H, Osmont A, Petit-Taboué MC, et al. Determination of ^{18}F -FDG brain kinetic constants in the anesthetized baboon. *J Neurosci Methods* 1993;50:263-272.
- Mazoyer BM, Huesman RH, Budinger TF, Knittel BL. Dynamic PET data analysis. *J Comput Assist Tomogr* 1986;10:646-653.
- Bendriem B, Soussaline F, Campagnolo R, Verrey B, Wajenberg P, Syrota A. A technique for the correction of scattered radiation in a PET system using time of flight information. *J Comput Assist Tomogr* 1986;10:287-295.
- Sette G, Baron JC, Young AR, et al. In vivo mapping of brain benzodiazepine receptor changes by positron emission tomography after focal ischemia in the anesthetized baboon. *Stroke* 1993;24:2046-2058.
- Koeppel RA, Holthoff VA, Frey KA, Kilbourn MR, Kuhl DE. Compartmental analysis of ^{11}C Flumazenil kinetics for the estimation of ligand transport rate and receptor distribution using positron emission tomography. *J Cereb Blood Flow Metab* 1991; 11:735-744.
- Logan J, Fowler JS, Vlokov ND, et al. Graphical analysis of reversible radioligand binding from time-activity measurements applied to $[\text{N-}^{11}\text{C-methyl}]\text{-}(-)\text{-Cocaine}$ PET studies in human subjects. *J Cereb Blood Flow Metab* 1990;10:740-747.
- Jobert A, Young AR, Suaudeau C, et al. Regional CBF, CBV, OEF and CMRO₂ values, their regional distribution, and their interrelationships in anaesthetized baboons: a PET investigation [Abstract]. *J Cereb Blood Flow Metab* 1991;11:S67.
- Perlmutter JS, Larson KB, Raichle ME, et al. Strategies for in vivo measurement of receptor binding using positron emission tomography. *J Cereb Blood Flow Metab* 1986;6:154-169.
- Frost JJ, Douglass KH, Mayberg HS, et al. Multicompartmental analysis of $[\text{N-}^{11}\text{C}]$ -

- carfentanil binding to opiate receptors in man measured by positron emission tomography. *J Cereb Blood Flow Metab* 1989;9:398–409.
29. Bevington PR. *Data reduction and error analysis for the physical sciences*. New York: McGraw-Hill; 1969:232–241.
 30. Mazoyer B. Investigation of the dopamine system with positron emission tomography: general issues in modelling. In: Baron JC, Comar D, Farde L, Martinot JL, Mazoyer B, eds. *Brain dopaminergic systems: imaging with positron tomography*. Dordrecht: Kluwer; 1991:65–83.
 31. Carson ER, Cobelli C, Finkelstein L. *The mathematical modelling of metabolic and endocrine systems*. New York: John Wiley; 1983:222.
 32. Yokoyama H, Yanai K, Inuma K, et al. Imaging of histamine H₁-receptors in human brain by PET analyzed by graphical analysis on a pixel-by-pixel basis [Abstract]. *J Cereb Blood Flow Metab* 1993;13(suppl 1):S796.
 33. Koeppe RA. Compartmental modeling alternatives for kinetic analysis of PET neurotransmitter receptor studies. In: Kuhl DE, ed. *In vivo imaging of neurotransmitter functions in brain, heart and tumors*. Washington, D.C.: American College of Nuclear Physicians; 1990:113–139.
 34. Delforge J, Loc'h C, Hantraye P, et al. Kinetic analysis of central ⁷⁶bromolisuride binding to dopamine D₂ receptors studied by PET. *J Cereb Blood Flow Metab* 1991;11:914–925.
 35. Huang SC, Barrio JR, Phelps ME. Neuroreceptor assay with positron emission tomography: equilibrium versus dynamic approaches. *J Cereb Blood Flow Metab* 1986;6:515–521.